HOW TO DO RF AT HIGH FIELDS

Tommy Vaughan, Lance DelaBarre, Carl Snyder, Mike Garwood, Gregor Adriany, Pat Bolan, Can Akgun, John Strupp, Peter Andersen, Pierre-Francois van de Moortele, Kamil Ugurbil

University of Minnesota Center for Magnetic Resonance Research
Minneapolis, MN, USA

INTRODUCTION

Human MR imaging to field strengths of 9.4T and higher appears to be possible according to recent data from the University of Minnesota. The Larmor wavelength in the human tissue dielectric at 400 MHz is on the order of 9cm. By conventional methods and thinking, this wavelength would preclude any possibility of achieving safe and successful human scale imaging. RF interference patterns from a conventional, uniform field volume coil would create severe inhomogeneities in the anatomic images. RF losses to the tissue conductor and the tissue dielectric at 400 MHz would result in increased heating concerns for conventional pulse protocols. Innovative methods and technology being developed at the University of Minnesota not only solve some of these problems, but actually use the short wavelengths to significant new advantages. By controlling the currents in individual RF coil elements, in phase, magnitude, frequency, and time, the RF field can be manipulated to optimize signal from a targeted region of interest for SNR, SAR, CNR, homogeneity, or other criteria. Such "B_1 shimming" will be automated much like magnetic field "B_0"shimming is today. A sampling of high frequency (RF) methods and technologies used for highest field human imaging will be presented and discussed

RF PROBLEMS

"High field" for human imaging currently ranges from 3T clinical imaging to 9.4T imaging research. The Larmor band for proton imaging over this span of field strengths ranges from 30 cm tissue wavelengths at 3T to 9cm wavelengths at 9.4T. Shortened wavelengths due to high tissue dielectric constants at high frequencies result in wave interference patterns with consequential RF field gradients and resultant image inhomogeneities over a field of view of human anatomic dimensions. Figure 1a models RF flux distortions through a head inside a homogeneous volume coil. Resulting RF field contours or gradients are shown in Figure 1b. Figure 1c shows the consequential B_1 inhomogenetiy in images acquired at 4T (1c) and 7T (1d) for a homogeneous TEM head coil. B_1 values were determined from the oscillation periods τ where $\Theta = \gamma B_1 \tau$, for a given B_1 generated by the RF coil. Averaged B_1 values standardized to a 1kW RF pulse are shown on the central and peripheral regions from which they were measured. (1-3)

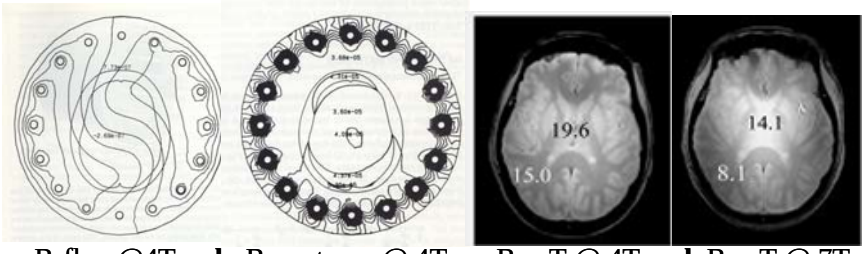

a. B_1flux @4T **b.** B_1contours @ 4T **c.** B_1,μT @ 4T **d.** B_1,μT @ 7T

Figure 1. 1a shows the calculated RF magnetic vector potential, Webers and 1b shows RF flux density (Webers/mm2). Figures 1c and 1d show B_1, μT in images at 4T and 7T

RF field dependent SAR and SNR also present problems at higher B_0 fields. As shown in Figure 2a, the RF power (SAR) required to excite a 90° flip angle increases with the B_0 field non-uniformly across the brain. This SAR increase may be linearly proportional to B_0 in the center of the brain, to quadratically proportional in the brain periphery with a homogeneous RF coil. Similarly, the signal-to-noise ratio (SNR) is also dependent on the B_1 contour as well as B_0, increasing at a better than linear proportion in the brain center and at a less than linear rate in the brain periphery when a homogeneous head coil is used. In Figure 2b, the SNR from five locations in a center slice of a fully relaxed gradient echo image acquired at 4T is compared to SNR values from the same slice acquired at 7T. The 7T image includes 7T/4T SNR ratios respective to the five locations as well. SAR and SNR as well as image homogeneity and contrast vary with the B_1 contours in the anatomy. (2)

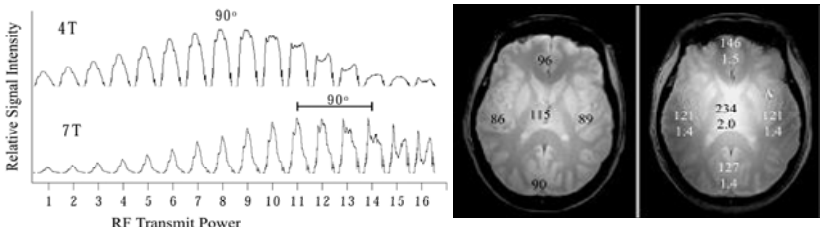

Figure 2a. Slice signal vs. power gain, dB **2b.** 4T signal 7T signal

RF SOLUTIONS

A variety of solutions exist for addressing the problems associated with MR imaging of human anatomy at high magnetic field strengths. Some proven approaches follow.

Image processing

The most obvious way to achieve uniform appearance of an image is to apply image signal intensity correction or other post signal acquisition processing algorithms. See Figure 3. While such image processing is commonly applied in most clinical imaging applications, this approach does not solve the fundamental RF problems associated with non-uniform B_1 contours discussed above. (2)

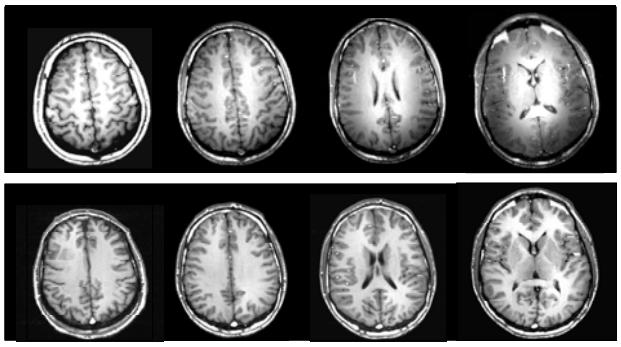

Figure 3. 7T images (a) intensity corrected (b)

Nested transmit coils and receive coils

Local transmit coils of conventional, circularly polarized birdcage or TEM design generate uniform, transverse B_1 fields. However, a high field human head image from such a coil used for both transmission and reception results in an inhomogeneous image with signal bias to the center of the head as described in Fig. 1. Alternatively, the sensitivity of close fitting receiver arrays favors the periphery of the head. By nesting a close fitting receive array together

a. Transmit coil **b.** Receive coil **c**. 4T image

Figure 4. A homogeneous transmit coil is nested with a local receive array to render apparent image homogeneity.

with a volume transmit coil, a more homogenous image can be achieved. (4,5) While apparently uniform images can be gained by super posing non uniform excitation and reception fields, optimal B_1 uniformity, SAR efficiency, and SNR are still compromised by this approach alone.

Multi-channel transmit and receive coils

Alternatively, transmit and receive coils can be designed such that the B_1 field of a coil can be optimized for image homogeneity or other criteria by controlling the RF currents on multiple, independent coil elements. One multi-channel design particularly well suited for high field use is the multi-channel TEM coil composed of transmission line elements which can be independently driven, controlled, and received efficiently at high frequencies. See Figure 5. (6)

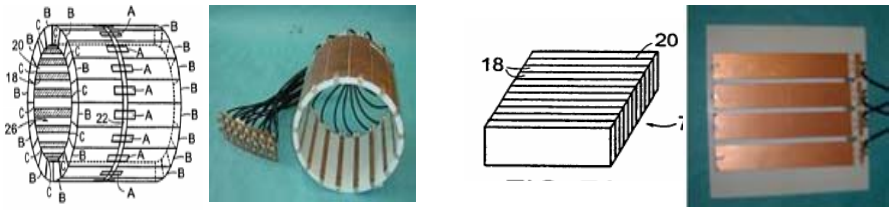

Figure 5a. Multi-channel TEM volume coil **5b.** Multi-channel TEM surface coil

Lines vs. loops

One choice to be made in multi-channel coil design is whether to use line elements or loop elements in the coil construction. While both element choices can be made more efficient by transmission line design, the line element is the shortest and therefore the most efficient. Optimization schemes are simplified with the uni-directional currents on the line elements. Line element or "runged" coils such and the birdcage and TEM resonators are inherently more homogeneous than loop arrays as well. See Figure 6. (7)

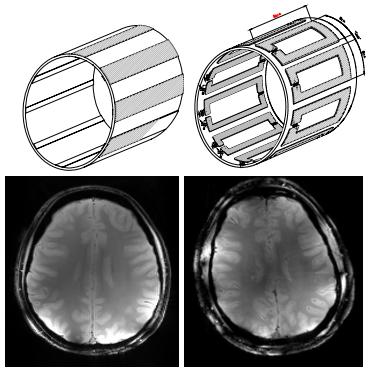

Figure 6. 7T images acquired with TEM line elements (left) and loop elements (right).

Design execution

Specific execution of any coil design can be used to determine performance criteria. For the multi-channel TEM volume coil, as with other designs, a closer fitting coil will improve the efficiency of transmission and reception. Interference patterns leading to image inhomogeneity are more extreme when elements are spaced closely to each other and to the anatomy. See Figures 7a, b. This problem can be lessened by the choice of dielectric material and dimension between the inner and outer conductors of the TEM elements, and by the number and dimension of elements. Homogeneity can be improved by making the coil physically larger, although at the expense of efficiency as in Figures 7c, d. Often compromising choices in geometry, material, ergonomics, implementation, and performance must be considered when designing a coil to for a specific application.

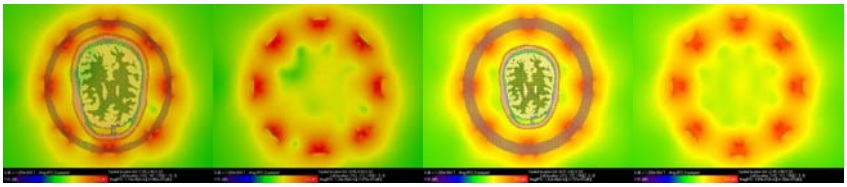

a. **b.** **c.** **d.**

Figure 7. B1 field models of a head loaded multi-channel TEM coil. 7a shows a close fitting coil with thin (blue circle) dielectric. 7c shows a thick dielectric with more spacious fit. 7b and 7d show respective models with head template removed for field visualization.

RF (B_1) SHIMMING

To control the phase, magnitude, timing and frequency of B_1 field generating currents on independent coil elements of multi-channel coils, multiple spectrometer transmit and receive channels are required. RF signals on each channel are independently modulated to effect the desired field control. This modulation is in turn controlled from the console by user interaction, programmed algorithms, or automated, feedback driven optimization protocols. See Figure 8.(8)

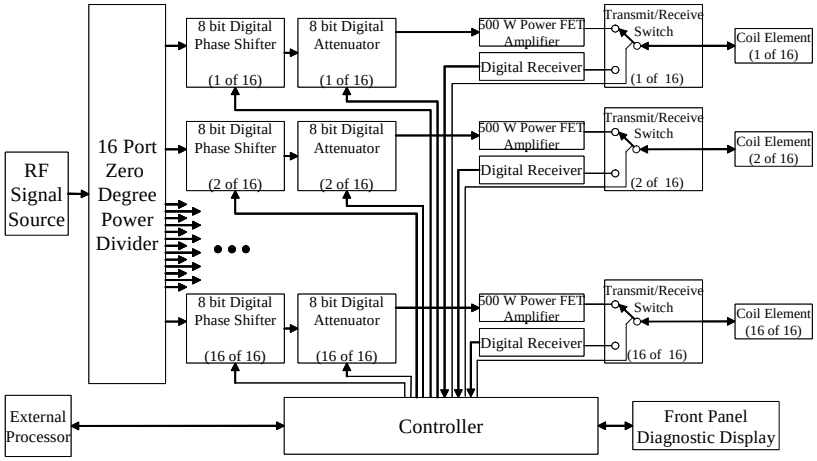

Figure 8. Functional schematic of a multi-channel, parallel transceiver to control B_1 transmit magnitude, phase, time (switching), and frequency per element of a multi-element coil.

APPLICATIONS

Head imaging

Results from the application of some of the RF solutions presented, follow. Figure 9 demonstrates B_1 shimming on a head at 9.4T. In this example, a multi-channel TEM volume coil per Fig 5a, designed by considerations of Fig 7a, was driven by the parallel transceiver of Fig 8. B_1 magnitude (top row) and B_1 phase (bottom row) were respectively optimized for best homogeneity. Phase and magnitude shimming were used together to produce the images of Figure 10. (9)

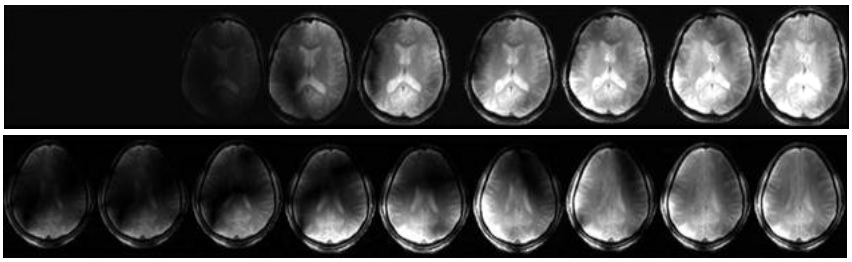

Figure 9. B_1 Shimming of head at 9.4T. Top row shows progressive shimming from left to right of B_1 magnitude. Bottom row shows shimming of B_1 phase.

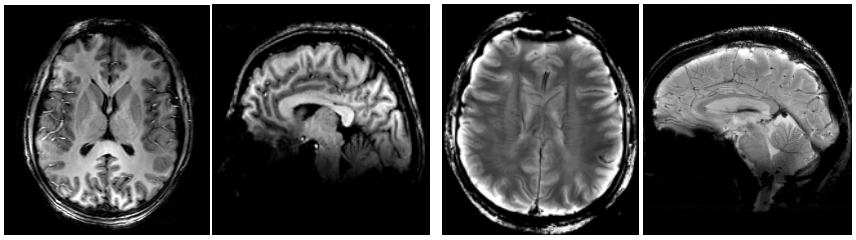

a. **b.** **c.** **d.**

Figure 10 a,b, show 9.4T gradient echo images acquired with the parallel transceiver driving an 8 channel transmit and receive, elliptical TEM head coil. The acquisition parameters were: TR/TE = 40/5ms, TI = 1.55 sec, Thk = 3mm, matrix = 256 x 128, SAR = 0.4W/kg. Simple magnitude addition was used to combine the images from eight receiver elements. No intensity correction was applied. **Figure 10 c,d**, show a 9.4T FLASH images, TR/TE = 50/9ms that contrast the medulary veins, Virchow-Robins spaces, possible tracts and other features.

Multi-nuclear imaging

Signal-to-noise and spectral resolution gains greatly benefit multi-nuclear NMR at high field strengths. By tuning alternating elements of a TEM coil to two frequencies, and transmitting and receiving at these two frequencies, multi-nuclear image acquisition can be simultaneously accomplished. See Figure 11. Alternatively frequency can be shifted per channel over time to acquire interleaved results in a "frequency hopping" scheme for two or more frequencies. (1,10)

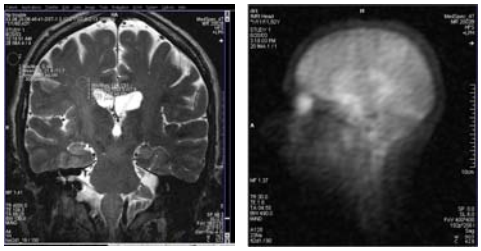

Figure 11. ^{1}H and ^{23}Na images from double tuned TEM coil at 4T. – courtesy, Bruker

Body imaging

The methods described herein for head imaging at high fields apply to full body imaging as well. Because human trunk dimensions are larger than in the head, significant RF artifacts become problematic at proportionately lower field strengths. The TEM body coil as shown in Figure 12 (a) was used together with two surface coil arrays (b) fitted to the chest and back of a volunteer to acquire the adjacent gated cardiac images at 4T. The RF artifact in the atrium of the left image was corrected by B_1 shimming as evidenced in the right image. (5)

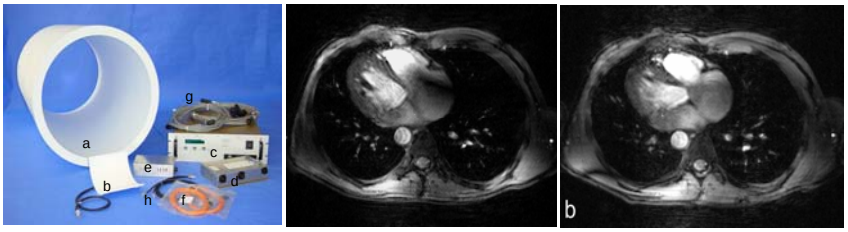

Figure 12. TEM Body Coil for 4T, 7T. The 4T cardiac image on the left shows an RF artifact in the right atrium. The image on the right shows the artifact removed by B_1 shimming.

For an initial mapping of the RF "landscape" in the body at 300 MHz (7T), coronal, saggital, and transaxial scout images were acquired with a TEM body coil as in Figure 12, activated in transmit and receive mode without the use of additional receiver coils. Limited at the time to a 4kW power amplifier, the parameters used for acquiring the gradient echo, whole body images of Figure 13 were: 256x256 matrix, 3mm thick slice, 2 ms windowed sinc pulse, flip angle = 25 degrees, TR/TE = 50/4 ms, 50 x 35 cm, NT = 2, scan time = 55 sec. These images show both RF problems and promise. Obvious are marked RF artifacts, especially the sharp destructive interference band (signal void) in the center of the trunk. Promising however is the surprising penetration through the trunk obtained with moderate SAR levels. Many of these artifacts were minimized or eliminated when receiver coils were used to localize specific ROIs. Work is now underway to employ B1 shimming with a new multi-channel TEM body coil to correct the remaining artifacts.

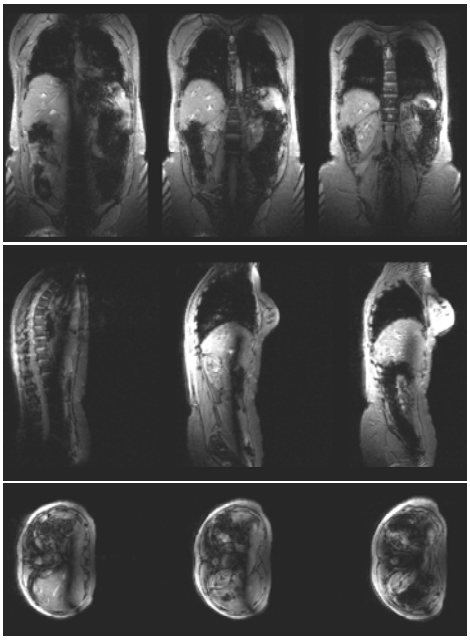

Figure 13. 7T Body Images. Can B_1 shimming correct these artifacts?

Localized imaging and spectroscopy

Whereas whole body imaging at the highest fields still presents some challenges, high quality images and spectra from localized regions of interest in the head, extremities, and superficial anatomy such as breasts can be easily measured with little complication. Breast cancer patient studies at 7T have been funded, approved, and are currently underway at the University of Minnesota.

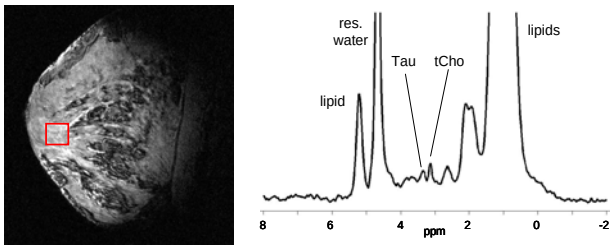

Figure 14. 7T Breast Image. The sagittal slice is from a fat-suppressed, T1-weighted 3D FLASH image acquired in a normal subject. The box indicates the voxel in the fibroglandular tissue from whence the spectra were obtained. Clear peaks from taurine and tCho are visible.

CONCLUSIONS

While improved SNR and spectral resolution have been realized for human studies to 9.4T, there are new high field related RF problems to be solved. The history of NMR however is rich with fortuitous paradoxes where anticipated high field artifacts have led to BOLD new solutions. RF artifacts due to extremely short brain and muscle tissue wavelengths of 12cm at 7T and 9cm at 9.4T will become the increasingly powerful RF shims and gradients used to localize ROIs and to optimize selected criteria therein by new families of RF protocols and feedback driven optimization algorithms. Shorter wavelengths bring the new ability to "steer" RF fields to targeted anatomies and acquisition mechanisms. New RF shimming, localization and optimization techniques will not only solve many of the RF problems encountered at high field strengths, but will further amplify the SNR benefit already gained.

ACKNOWLEDGEMENTS

NIH-P41 RR08079, NIH-S10 RR139850, NIH-R01 CA94200, NIH-R33 CA94318, NIH- R01 EB000895-04, KECK Foundation.

REFERENCES

1. Vaughan J, Hetherington H, Otu J, Pan J, Pohost G. High frequency volume coils for clinical nuclear magnetic resonance imaging and spectroscopy. Magn Reson Med 1994;32:206-218.
2. Vaughan J, Garwood M, Collins C, DelaBarre L, Adriany G, Andersen P, Merkle H, Smith M, Ugurbil K. 7T vs. 4T: RF power, homogeneity & signal-to-noise comparison in head images. Magn Reson Med 2001;46:24-30.
3. Van de Mortele P-F, Akgun C, Adriany G, Moeller S, Ritter J, Collins C, Smith M, Vaughan J, Ugurbil K. B1 destructive interferences and spatial phase patterns at 7 tesla with a head transceiver array coil. Magn Reson Med 2005.
4. Vaughan J, Adriany G, Garwood M, Yocoub E, Duong T, Merkle H, Andersen P, DelaBarre L, Kim S-G, Ugurbil K. A Detunable Volume Coil for High Field NMR. Magn Reson Med 2002;47:990-1000.
5. Vaughan J, Adriany G, Snyder C, Tian J, Thiel T, Bolinger L, Liu H, DelaBarre L, Ugurbil K. Efficient high-frequency body coil for high-field MRI. Magn Reson Med 2004;52:851-859.
6. Vaughan J; Massachusetts General Hospital, assignee. RF coil for imaging system. USA patent 6,633,161. 2003.

7. Adriany G, Van de Mortele P-F, Wiesinger F, Moeller S, Strupp J, Andersen P, Snyder C, Zhang X, Chen W, Pruessmann K, Boesiger P, Vaughan J, Ugurbil K. Transmit and receive transmission line arrays for 7 tesla parallel imaging. Magn Reson Med 2005;53:434-445.
8. Vaughan J, Adriany G, Ugurbil K, Strupp J, Andersen P; University of Minnesota, assignee. Parallel Transceiver for Nuclear Magnetic Resonance System. USA patent 6,969,992. 2005.
9. Vaughan T, DelaBarre L, Snyder C, Tian J, Bolan P, Garwood M, Adriany G, Strupp J, Andersen P, Van de Moortele P-F, Ugurbil K. Highest field human MR imaging. IEEE Transactions on EMC 2006:213.
10. Vaughan J; University of Alabama, Birmingham, assignee. High frequency volume coils for nuclear magnetic resonance applications USA patent 5,557,247. 1996.